ISSN 0021-3640, JETP Letters, 2019, Vol. 110, No. 9, pp. 607–612. © Pleiades Publishing, Inc., 2019.
Russian Text © The Author(s), 2019, published in Pis'ma v Zhurnal Eksperimental'noi i Teoreticheskoi Fiziki, 2019, Vol. 110, No. 9, pp. 607–613.

CONDENSED MATTER

# Complex Dynamics of the Cascade of Kink–Antikink Interactions in a Linear Defect of the Electroconvective Structure of a Nematic Liquid Crystal

**V. A. Delev[a, *], V. N. Nazarov[a, b], O. A. Scaldin[a], E. S. Batyrshin[c], and E. G. Ekomasov[c, d, e]**

[a] *Institute of Molecule and Crystal Physics, Ufa Federal Research Centre, Russian Academy of Sciences, Ufa, 450075 Russia*

[b] *Bashkir State Medical University, Ufa, 450008 Russia*

[c] *Bashkir State University, Ufa, 450076 Russia*

[d] *University of Tyumen, Tyumen, 625003 Russia*

[e] *South Ural State University (National Research University), Chelyabinsk, 454080 Russia*

**e-mail: delev@anrb.ru*

Received July 8, 2019; revised October 7, 2019; accepted October 8, 2019

The complex dynamics of an ensemble of dislocations in a linear defect appearing in a one-dimensional electroconvective structure of a $\pi/2$-twisted nematic liquid crystal has been studied. This type of defects is characterized by a quite extended strain field or degree of "dissociation." Hydrodynamic flows in domains of the twisted nematic liquid crystal have not only the tangential velocity component but also the axial component whose directions in neighboring domains are opposite. Under the action of an applied voltage, the linear defect with the topological charge $S = -1$ begins to oscillate and decays into an odd number of dislocations with the conservation of the total topological charge. The further dynamics of dislocations in the core of the defect is established such that it ensures the continuity of the flow of an anisotropic liquid in domains. The spatiotemporal dynamics of the cascade of interacting dislocations is qualitatively well described by the multikink solution of the sine-Gordon equation. The fundamental possibility of creating new model objects with a given number of interacting dislocations has been shown.

**DOI:** 10.1134/S0021364019210069

Transition from an ordered state to spatiotemporal chaos in nonequilibrium systems is often accompanied by the formation of defects [1, 2]. Despite significant differences in the physical properties of systems (Bénard–Marangoni convection, Couette–Taylor flow, electroconvection in liquid crystals, etc.), the dynamics of topological defects, which are analogs of edge dislocations in crystals, has many common features. In particular, it was shown that the number of defects increases when exceeding supercriticality and defects can form bound states, domain walls, etc. [3]. For this reason, the study of the dynamic characteristics of defects and their role in the appearance of turbulence in nonequilibrium systems is one of the important problems of condensed matter physics.

To understand the complex dynamics of an ensemble of interacting dislocations, it is first necessary to study the properties and behavior of individual defects. However, it is quite difficult to experimentally obtain individual defects and to analyze their properties in isotropic liquids. This can be reached in an appropriate model system of electroconvection in a nematic liquid crystal because it has an axial anisotropy characterized by a unit vector **n** called director [4–6].

Defects in liquid crystals can appear under certain conditions at both microscopic (molecular) and macroscopic (period of a structure) scales. Their topological (static) properties are very similar and studied in detail [7–11], whereas dynamic characteristics remain poorly studied. The existing works are mainly devoted to defects of electroconvective structures in a nematic liquid crystal with the planar orientation of the director **n** [12–17]. The results of these works indicate an important role of defects in the complication of the spatiotemporal dynamics of electroconvective structures and in processes of their turbulization at an increase in the applied voltage. It has been established that processes of creation and annihilation of dislocations are the most general mechanisms at the formation of two-dimensional lattices. The behavior of dislocations in the weak supercriticality approximation is well described by the Ginzburg–Landau equation [15–17].

As shown in [17], at a certain rate of increase in the applied voltage, dislocations can form a new localized quasistationary state in the space with a lower symmetry. Such a state is usually nucleated near the core of a dislocation and propagates along a line normal to Williams domains. The appearing *linear defect* with a dissociated ("extended") core has the same topological charge as the initial dislocation. Furthermore, a localized state can be spontaneously formed because of the development of modulation instability as a simple shift of domains along lines (normal to Williams domains) by half of the spatial period $\pi$ without the formation of dislocations. Consequently, such a distortion of the domain structure is not a defect in the topological sense and was called the *phase jump line* [17].

The indicated types of linear objects in electroconvective structures of nematic liquid crystals with the planar orientation of the director **n** become unstable under fast variation of the applied voltage [17]. As a result, linear defects decay into an odd number (no less than three) of dislocations, whereas phase jump lines decay into an even number (no less than two) of dislocations with opposite topological charges $S = +1$ and $-1$. The total topological charge is conserved in both cases.

Similar linear localized deformations are also observed in electroconvective structures of twisted nematic liquid crystals [18–21]. However, they are quite stable because of the features of hydrodynamic flows considered below. A slow increase in the applied voltage is accompanied by an increase in their length $L$, which can reach the size of the liquid crystal sample. In this case, the superposition of Williams domains and linear objects normal to them results in the formation of a quasistationary two-dimensional structure [18, 20]. At a fast increase in the voltage, domain zigzag oscillations first appear in quasistationary linear objects and dislocations separating zig and zag regions are then formed.

The dynamics of dislocations in localized objects depends on the length and type of these objects. In particular, the periodic creation and annihilation of two dislocations with topological charges $S = +1$ and $-1$ occur on the phase jump line with the length $L = 8\lambda$, where $\lambda$ is the transverse size of the domain [22]. In another case, where the length of the line is $L = 14\lambda$, after the appearance of oscillations on it, the generation of a dipole pair of dislocations occurs on one end of the line, whereas their annihilation proceeds on the other end. Such an oscillatory dynamics of dislocations is qualitatively well described by the localized breather solution of the sine-Gordon equation [23].

However, the situation changes significantly if a linear defect with a sufficiently extended strain field is experimentally implemented. On one hand, the motion of dislocations and, correspondingly, topological solitons in model representation can be considered as quasifree. On the other hand, there is a problem of the character and type of the interaction between them. In particular, we showed in [24] that the collision of dislocations in an extended defect can be treated as a bound state of a kink and an antikink of the sine-Gordon equation.

In this work, we analyze a more complex motion and interaction of dislocations when dipole pairs of dislocations are periodically created on both edges of an extended defect in the electroconvective structure of a nematic liquid crystal with the initial $\pi/2$-twisted orientation of the director field **n**.

As a nematic liquid crystal, we used 4-*n*-methoxybenzylidene-*n*-butylaniline (MBBA), which was placed in a liquid crystal cell between two glass substrates with a $SnO_2$ conducting coating. The surface of the substrates with electrodes was covered with an AL1254 polyimide film (JSR Corp., Japan). This film was then rubbed in one direction to create a uniform planar orientation of the director **n**. The thickness of the 16 × 12-mm liquid crystal cell was specified by 20-μm Mylar spacers. After the cell was filled with the nematic liquid crystal and a uniform planar orientation was formed, the upper substrate was rotated slowly with respect to the lower substrate clockwise by an angle of $\pi/2$. As a result, a uniformly twisted orientation of the director **n** appeared in the entire nematic liquid crystal layer. An alternating voltage $U$ with the frequency $f_U = 30$ Hz was applied to the liquid crystal layer. The threshold voltage of the appearance of Williams domains was $U_c = 5.6$ V. The axis of these domains was perpendicular to the midplane director **n** of the nematic liquid crystal layer and made angles of $-45°$ and $45°$ with the orientations of the director on the upper and lower substrates, respectively. The directions of hydrodynamic flows in the domains were determined by analyzing the motion of probe particles 2–3 μm in diameter introduced in the nematic liquid crystal. Domain structures and their defects were observed in an Axiolab polarization microscope (Zeiss, Germany) and their images were recorded by a VX44 video camera (PCO Inc., Germany) with a resolution of 720 × 576 pixels and were digitized by an external Pinnacle 700-USB analog-to-digital converter (United States).

Domains of the one-dimensional electroconvective structure in the nematic liquid crystal are cylindrical convective objects—walls (or rolls) similar to those formed in isotropic thermal convection. A defect with the topological charge $S = +1$ and $-1$ (dislocation) corresponds to the phase jump of $+2\pi$ and $-2\pi$, respectively, in the structure of Williams domains; i.e., its singularity is determined by the extra (or missing) spatial period at the bypass of a closed contour around its core [12].

We consider the structure of the linear defect with the dissociated core in the domain structure of the twisted nematic liquid crystal taking into account the features of hydrodynamic flows (Fig. 1). Unlike the planar oriented nematic liquid crystal, convective flows in the domain structure of the twisted nematic liquid crystal have not only the tangential velocity

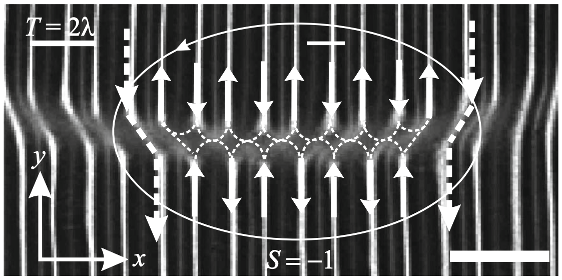


**Fig. 1.** Image of the linear defect with the dissociated core in the domain structure of the twisted nematic liquid crystal at $U = 6.5$ V and $f = 30$ Hz. Arrows show the directions of the axial velocity components of convective flows $v_a$ in domains near the defect core. Thin dashed lines indicate the redistribution of flows in the defect core. White lines correspond to the centers of domains around which the helicoidal motion of particles is observed. A scale of 100 μm is given by the horizontal straight segment in the lower right corner of the figure.

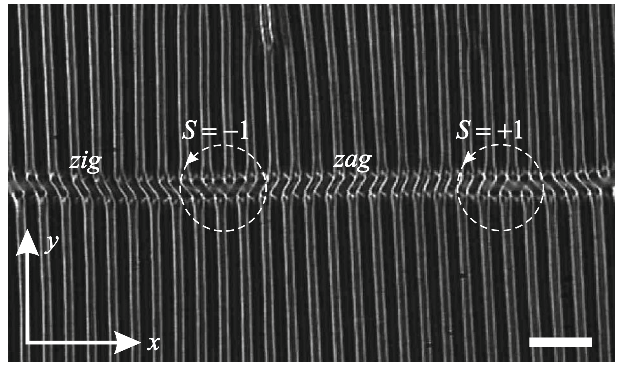


**Fig. 2.** Image of the domain structure with an extended defect in the twisted nematic liquid crystal at $U = 7.6$ V and $f = 30$ Hz. A scale of 100 μm is given by the horizontal straight segment in the lower right corner of the figure.

component $v_t$ but also the axial component $v_a$ whose directions in neighboring domains are opposite [25]. For this reason, the flow of the anisotropic liquid in domains becomes helicoidal and the spatial period of the structure is $T = 2\lambda$. Observations of probe particles show that the continuity of flows in the defect is ensured both by the closure of codirected axial velocity components $v_a$ through the core and by their closure with oppositely directed flows in neighboring domains (Fig. 1). At voltages $U \leq 7.4$ V, convective flows in domains are steady.

Both velocity components $v_t$ and $v_a$ of the flow of the anisotropic liquid in domains increase with the applied voltage and the linear defect becomes unstable at $U > 7.4$ V. However, in contrast to the planar oriented nematic liquid crystal [17], the core of the defect does not decay into separate dislocations, but first begins to oscillate. In this case, the successive (time-periodic) reconnection of domains with codirected flows of the anisotropic liquid to the left (*zig*) and to the right (*zag*) is observed and the motion of the liquid in the core of the defect becomes pulsatory. Then, the core of the defect decays into zig and zag regions oscillating out-of-phase. Dislocations with the topological charges $S = +1$ and $-1$ are simultaneously formed between the boundaries of zig and zag regions (Fig. 2).

The further dynamics of dislocations is established such that it ensures the continuity of the helicoidal flow of an anisotropic liquid in the core of the nonstationary defect. Since the length of the defect $L$ and, consequently, the number of dislocations depend on the applied voltage, it is possible in principle to experimentally implement an extended defect with a given number of interacting dislocations. Thus, the extended oscillating defect can be considered as a one-dimensional model object for studying the motion and interaction of dislocations.

Images of electroconvective structures in the nematic liquid crystal represent spatially periodic modulations of the intensity of light transmitted through the cell with the nematic liquid crystal. These modulations correspond to local changes in the optical anisotropy $\langle \Delta n(t) \rangle$ under the action of the external electric field. Hydrodynamic convective motions in the form of walls (or rolls) are excited in the nematic liquid crystal layer at the electroconvection threshold. The convective motion particularly strongly orients the nematic liquid crystal in the region of the maximum velocity gradient, i.e., in the center of vortices. As a result, cylindrical vortices serve as lenses focusing light in white lines, domains [26], and form an image in the form of black and white stripes (Fig. 2).

Thus, the intensity distribution $I(x, y)$ in the initial image of the structure has a clear spatial periodicity in the $xy$ plane of the liquid crystal sample. The vertical stripes correspond to stationary domains, whereas the extended defect is represented by a horizontal stripe formed by oblique zig and zag domains. Since the wave vectors of vertical and oblique domains are obviously different, their contributions to the resulting image of the structure can be easily separated using a two-dimensional Fourier transform. This principle underlies the spatial demodulation technique [27], which makes it possible to obtain the spatial distribution of the amplitude of this periodicity from the initial image $I(x, y)$ of the periodic structure. This amplitude characterizes the difference in the intensity between black and white stripes in the image. Correspondingly, zero amplitude indicates the absence of a periodic structure. In this case, we are interested in the amplitudes $A_{\text{zig}}(x, y)$ and $A_{\text{zag}}(x, y)$ of oblique zig and zag domains in the core of the defect, respectively (Fig. 2). After the successive demodulation of each image of the video sequence $I(x, y, t)$ (Fig. 3a, upper part), spatiotemporal dependences of the difference of the amplitudes $A_{\text{zig}}(x, y, t)$ and $A_{\text{zag}}(x, y, t)$ were obtained in

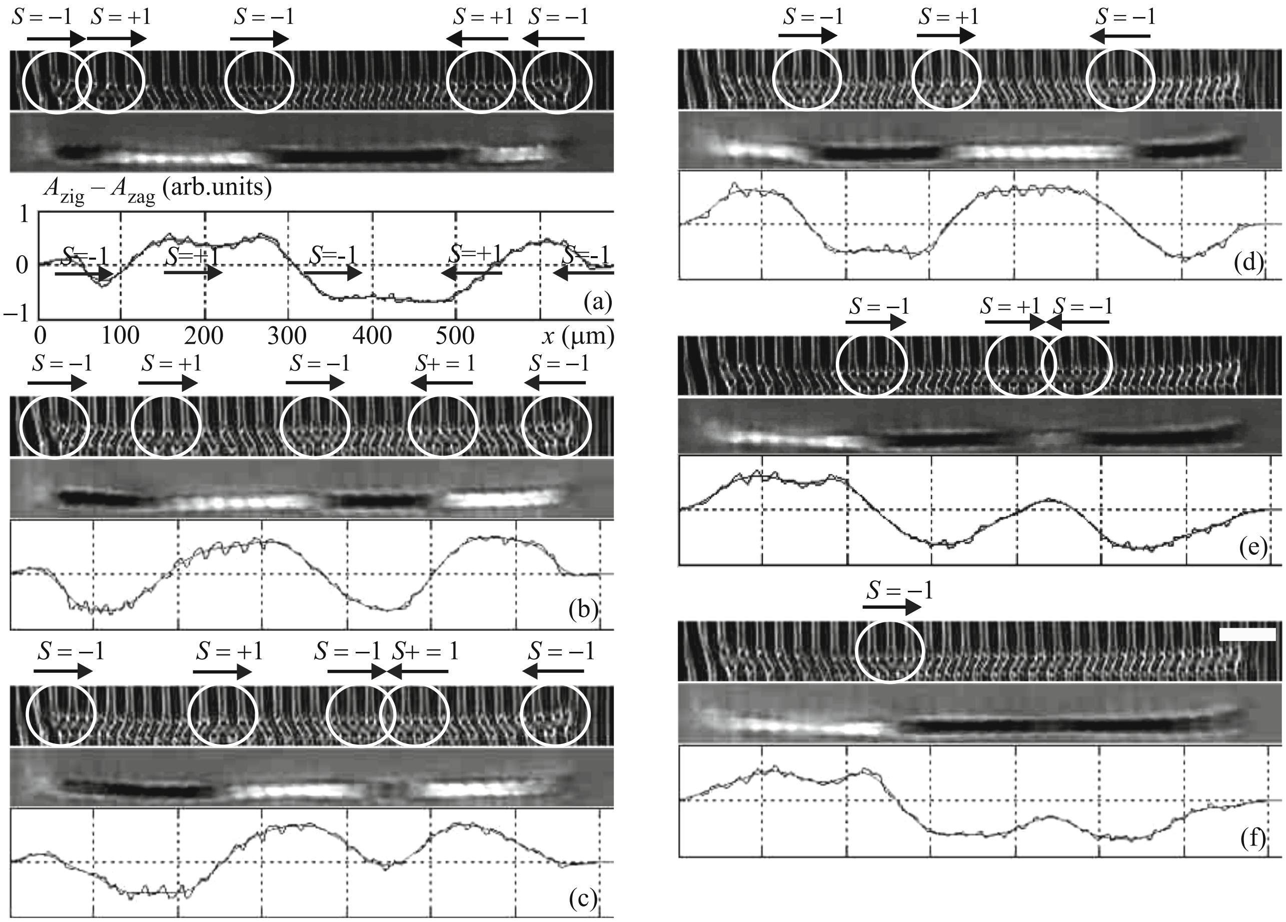


**Fig. 3.** Dynamics of the cascade of interacting dislocations with $S = +1$ and $-1$ in the linear defect at $U = 7.6$ V during one oscillation period $T = 1.2$ s. (a–f) (Upper part) Initial image of the linear defect, (middle part) demodulated half-tone image of the difference of the amplitudes of oblique domains, and (lower part) amplitude difference $A_{zig}(x,t) - A_{zag}(x,t)$ at $\Delta t = 0.24$ s. A scale of 100 μm is given by the horizontal straight segment in the lower right corner of the figure.

the form of half-tone images (Fig. 3a, middle part). In these images, the zig mode (domains inclined to the left) corresponds to the white region, whereas the zag mode (domains inclined to the right) corresponds to the black region. The boundaries of the transformation of the white region to the dark one (or vice versa) in the demodulated image indicate the localization of dislocations with $S = -1$ (or $S = +1$). Then, the amplitude differences were averaged over $y$ near the core of the defect. The resulting plots $A_{zig}(x, t)$ and $A_{zag}(x, t)$ (Fig. 3a, lower part) were used to analyze the dynamics of dislocations. In this case, the localization of dislocations is indicated by the points of intersection of the curve with the zero horizontal axis.

We analyze in detail the dynamics of the cascade of interacting dislocations in the linear defect with a length of about 30 spatial periods of the domain lattice (Fig. 3).

Let the linear defect with the topological charge $S = -1$ at the initial time $t = 0$ be in the steady state. As the voltage in the core of the defect increases, oblique zig and zag domains are formed together with a dislocation between them, which moves to the right. The state of the defect at this time is similar to that shown in Fig. 3f. Two dipole pairs of dislocations with $S = \mp 1$ (at the left edge) and with $S = \pm 1$ (at the right edge) are created simultaneously at both edges of the defect (Fig. 3a). Thus, five dislocations are located in the core of the defect. Two dislocations—the second dislocation on the left with $S = +1$ and the central one with $S = -1$—move to the right, whereas the second dislocation on the right with $S = +1$ moves to the left (Fig. 3b). The extreme dislocations remain immobile. Figure 3c shows the beginning of the interaction between the nearest counterpropagating dislocations—the central dislocation with $S = -1$ and the second one on the right with $S = +1$. The extreme dislocations with $S = -1$ remain at the edges of the defect. Further, simultaneously with the annihilation of interacting dislocations at the point with the coordinate $x \simeq 440$ μm, the extreme dislocations with the topological charge $S = -1$ begin to move (Fig. 3d). Then, the interaction of two dislocations occurs again: the second dislocation on the left with the topological charge $S = +1$ interacts with the dislocation remaining on the right with the topological charge $S = -1$ (Fig. 3e). After its annihilation at the same point $x \simeq 440$ μm, one dislocation with the topological charge $S = -1$ holds (Fig. 3f) and the process repeats again.

We now try to qualitatively describe the observed dynamic process within the sine-Gordon model [28]. Since the size of the unit cell of the electroconvective structure in the π/2-twisted nematic liquid crystal is defined as $T = 2\lambda$ because the axial components of the flow velocity in neighboring domains are antiparallel, we will consider the center of the "dislocation" along the $x$ direction as a site of the domain lattice. Then, as shown in [21, 22], the equation of motion after the transition to the continual approximation has the form

$$\frac{\partial^2\eta}{\partial\tau^2} - \frac{\partial^2\eta}{\partial\xi^2} + \beta\sin\eta = 0. \tag{1}$$

Here, $\eta = \pi u/\lambda$ is the dimensionless displacement function of the double domain from its equilibrium position along the $x$ direction; $\xi = x/(2\lambda\sqrt{\tilde{k}})$ is a dimensionless coordinate, where $\tilde{k} = (\lambda/\pi)^2(k'/V_0')$, $k'$ is the coupling constant of neighboring domains, and $V_0'$ is the energy per unit length of the double domain; $\tau = (\pi/\lambda)\sqrt{V_0'/m'}t$ is the dimensionless time, where $m' = m/l$ is the specific mass of the double domain and $l$ is the length of the double domain; and the parameter $\beta$ is a function of the coordinates in the form of a "potential well"; for simplicity, we set $\beta = 1$.

To describe the experimental results, we use the kink (antikink) solutions of Eq. (1) in the form [29]

$$\eta = 4\arctan\left(\exp\left(\pm\frac{\xi - \xi_0 - v\tau}{\sqrt{1 - v^2}}\right)\right), \tag{2}$$

where $\xi_0$ is the coordinate of the center of the kink with respect to their interaction point and $v$ is its velocity.

Further, assuming that the collision of dislocations in the experiment can be treated as the kink–antikink interaction (see, e.g., [24]), we apply Eqs. (1) and (2) to the studied problem. The solution of Eq. (1) is taken in the form of a chain of kinks and antikinks with opposite topological charges $S = +1$ and $-1$. We take an odd number of kinks: three on the left (two antikinks and one kink) and two on the right (kink and antikink). Let kinks and antikinks at the initial time be spaced by a certain distance corresponding to experimental data (Fig. 3). The place of collision of kinks and antikinks (origin of the coordinate system), which is a potential well, is considered as the center of the system under study. Such a kink–antikink interaction can be dynamically considered as a breather of the sine-Gordon equation localized in the well [30]. Such groups consisting of kinks and antikinks with opposite topological charges move toward each other at different dimensionless velocities. The numerical experiment indicates that the theory is in agreement with the experiment if the kinks on the right are ~30% wider than the kinks on the left.

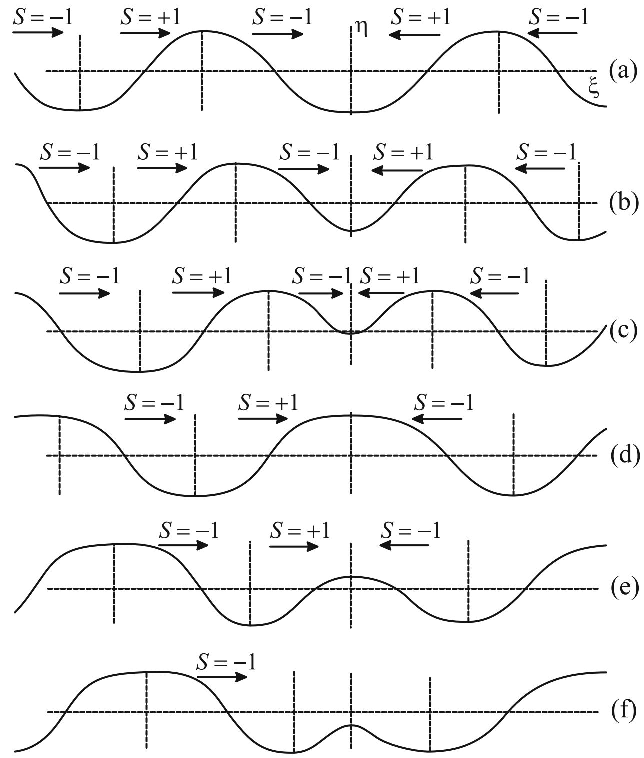


**Fig. 4.** Numerical illustrations of the dynamics of the cascade of kink–antikink interactions at different times.

Figure 4 shows the dependences of the form of the solution of Eq. (2) for the cascade of kink–antikink interactions at different times. In the numerical calculations, we used the experimentally obtained dimensionless velocities of dislocations $v_1 = 0.36$ and $v_2 = 0.3$, which are ratios of the absolute velocities of dislocations $V_1 \simeq 180$ μm/s and $V_2 \simeq 150$ μm/s at a given voltage of $U = 7.6$ V to the average maximum velocity of their motion $\langle V_{\max}\rangle \simeq 500$ μm/s for $U = 10$ V, at which the domain structure is still stationary.

The comparison of theoretical dependences (Fig. 4) with experimental curves (Fig. 3) shows a good qualitative correlation between the results.

To summarize, the spatiotemporal dynamics of the ensemble of interacting dislocations in the linear defect of the electroconvective structure of the π/2-twisted nematic liquid crystal has been analyzed.

The motion and interaction between dislocations in the core of the defect are established such that they ensure the continuity of the flow of the anisotropic liquid in domains. It has been shown that the dynamics of dislocations in the linear defect is qualitatively well described by the multikink solution of the sine-Gordon equation. The studied extended defects can be considered as one-dimensional model objects for studying the complex dynamics of dislocations.

## ACKNOWLEDGMENTS

The experiments were performed using equipment of the Shared Use Center Spectr, Institute of Molecular and Crystal Physics, Ufa Federal Research Centre, Russian Academy of Sciences, and the Regional Shared Use Center Agidel.

## FUNDING

This work was performed within the state assignment no. AAAA-A19-119022290052-9. E.G.E. acknowledges the support of the Government of the Russian Federation (agreement no. 02.A03.21.0011, decision no. 211 on March 16, 2013).

## REFERENCES

1. P. Coullet, L. Gil, and J. Lega, Phys. Rev. Let. **62**, 2957 (1989).
2. M. I. Rabinovich and M. M. Sushchik, Sov. Phys. Usp. **33**, 1 (1990).
3. M. C. Cross and P. C. Hohenberg, Rev. Mod. Phys. **65**, 851 (1993).
4. S. A. Pikin, *Structural Transformations in Liquid Crystals* (Nauka, Moscow, 1981; Gordon and Breach Science, New York, 1991).
5. P. G. de Gennes and J. Prost, *The Physics of Liquid Crystals* (Clarendon, Oxford, 1994).
6. A. Buka and L. Kramer, *Pattern Formation in Liquid Crystals* (Springer, New York, 1996).
7. M. Kleman, *Points, Lines and Walls in Liquid Crystals, Magnetic Systems and Various Ordered Media* (Wiley, Chichester, 1983).
8. M. V. Kurik and O. D. Lavrentovich, Sov. Phys. Usp. **31**, 196 (1988).
9. L. Lam and J. Prost, *Solitons in Liquid Crystals* (Springer Science, New York, 1992).
10. O. D. Lavrentovich, P. Pasini, S. Zannoni, and S. Zumer, *Defects in Liquid Crystals: Computer Simulations, Theory and Experiments* (Kluwer Academic, The Netherlands, 2001).
11. P. V. Dolganov, V. M. Zhilin, V. K. Dolganov, and E. I. Kats, JETP Lett. **89**, 161 (2009).
12. A. Joets and R. Ribotta, J. Phys. (Paris) **47**, 595 (1986).
13. S. Kai, N. Chizumi, and M. Kohno, J. Phys. Soc. Jpn. **58**, 3541 (1989).
14. S. Nasuno, S. Takeuchi, and Y. Sawada, Phys. Rev. A **40**, 3457 (1989).
15. S. Rasenat, V. Steinberg, and I. Rehberg, Phys. Rev. A **42**, 5998 (1990).
16. E. Bodenschatz, W. Pesch, and L. Kramer, J. Stat. Phys. **64**, 1007 (1991).
17. A. Joets and R. Ribotta, J. Stat. Phys. **64**, 981 (1991).
18. V. A. Delev, P. Toth, and A. P. Krekhov, Mol. Cryst. Liq. Cryst. **351**, 179 (2000).
19. O. A. Skaldin, G. R. Yakupova, V. A. Delev, Yu. A. Lebedev, and A. A. Nazarov, Phys. Solid State **47**, 374 (2005).
20. S. Tatsumi, M. Sano, and A. G. Rossberg, Phys. Rev. E **73**, 011704 (2006).
21. A. N. Chuvyrov, O. A. Scaldin, V. A. Delev, Yu. A. Lebedev, and E. S. Batyrshin, J. Exp. Theor. Phys. **103**, 926 (2006).
22. O. A. Scaldin, V. A. Delev, E. S. Shikhovtseva, E. S. Batyrshin, and Yu. A. Lebedev, JETP Lett. **93**, 388 (2011).
23. O. A. Scaldin, V. A. Delev, E. S. Shikhovtseva, Yu. A. Lebedev, and E. S. Batyrshin, JETP Lett. **100**, 162 (2014).
24. V. A. Delev, O. A. Scaldin, E. S. Batyrshin, V. N. Nazarov, and E. G. Ekomasov, JETP Lett. **109**, 87 (2019).
25. A. Hertrich, A. P. Krekhov, and O. A. Scaldin, J. Phys. II (France) **4**, 239 (1994).
26. L. M. Blinov, *Electro-Optical and Magneto-Optical Properties of Liquid Crystals* (Nauka, Moscow, 1978; Wiley, Chichester, 1983).
27. M. Dennin, D. S. Cannell, and G. Ahlers, Phys. Rev. E **57**, 638 (1998).
28. O. M. Braun and Yu. S. Kivshar, *The Frenkel—Kontorova Model: Concepts, Methods, and Applications* (Springer, Berlin, 2004).
29. A.-M. Wazwaz, *Partial Differential Equations and Solitary Waves: Theory* (Springer, Dordrecht, Heidelberg, London, New York, 2009).
30. J. Cuevas-Maraver, P. G. Kevrekidis, and F. Williams, *The Sine-Gordon Model and Its Applications. From Pendula and Josephson Junctions to Gravity and High-Energy Physics* (Springer, Heidelberg, New York, Dordrecht, London, 2014).

*Translated by R. Tyapaev*